Available online at www.sciencedirect.com
ScienceDirect
Ceramics International 35 (2009) 2921–2926
CERAMICS INTERNATIONAL
www.elsevier.com/locate/ceramint

Representation of thermal conductivity of solid material with particulate inclusion

Yoshihiro Hirata *

Department of Advanced Nanostructured Materials Science and Technology, Kagoshima University, 1-21-40 Korimoto, Kagoshima 890-0065, Japan

Received 28 February 2009; received in revised form 12 March 2009; accepted 30 March 2009
Available online 24 April 2009

Abstract

This paper reviewed the previously proposed models of thermal conductivity (κ) for a series and parallel flow of energy input in laminated composites. These two models were coupled to derive the thermal conductivity (κ_a) of material with simple cubic particulate inclusion. The derived equation depends upon κ_1 of inclusion, κ_2 of a continuous phase and volume fraction of inclusion. The size and shape factors of inclusion are cancelled during the derivation of κ_a. The newly constructed κ_a equation explains well the measured κ_a for AlN particle-dispersed SiO_2 system.

Keywords: A. Hot pressing; B. Inclusions; C. Thermal conductivity; D. Nitrides

1. Introduction

Thermal conductivity is an important property of material, which is used to design a structure of assembly of functional parts or to estimate a temperature gradient in the material at a given energy flux. Fortunately many thermal conductivities of metal and ceramics are available in Chemical Handbook [1] or Metal Handbook [2]. In a previous paper [3], a wide variety of thermal conductivity (κ) of metal and ceramics is discussed with a harmonic oscillator model of lattice vibration. The theoretical approach succeeded in representing κ with atomic weight, Young's modulus (E) and density (ρ). The E and ρ values are closely related to the nature of chemical bond (metallic, covalent and ionic bonds). A very good agreement is observed between the measured and calculated κ values in the wide range from 1 to 2310 J/smK. The next interesting observation is the theoretical expression of thermal conductivity for the material with inclusion (second phase or pore). In this paper, two simple models with plates of different κ values are coupled to derive κ_a for the material with particulate inclusion. The derived κ_a can be expressed with three parameters of κ_1 for inclusion, κ_2 for a continuous phase and volume fraction (V) of inclusion. The dependence of κ_a on volume fraction of inclusion is compared with the experimentally measured κ_a for AlN–SiO_2 system [4,5]. The thermal diffusibility (α, m^{-2}) of AlN–SiO_2 hot-pressed at 1400–1600 °C in a N_2 atmosphere was measured at room temperature at Dow Chemical International Ltd., Research & Development Laboratory, Midland, USA, and converted to a thermal conductivity using the specific heat of 0.736 (pure AlN)–0.841 (pure silica) J/gK [4].

2. Steady-state analysis of thermal conductivity

The equation of heat conduction along x direction in Fig. 1 is given by Eq. (1),

$$\frac{\partial T}{\partial t} = \alpha \frac{\partial^2 T}{\partial x^2} \tag{1}$$

where T is the temperature and α the thermal diffusibility (1/m^2). The steady-state condition is $\partial T/\partial t = 0$ and the temperature gradient along x direction ($\partial T/\partial x$) becomes a constant value. On the other hand, thermal conductivity (κ) is defined by Eq. (2),

$$I = \kappa \frac{\mathrm{d}T}{\mathrm{d}x} \tag{2}$$

where I is the flux of energy (J/sm^2) input in a material with thickness L in Fig. 1. Since the temperature gradient is constant at the steady-state condition, the I/κ ratio becomes a constant

* Tel.: +81 99 285 8325; fax: +81 99 257 4742.
E-mail address: hirata@apc.kagoshima-u.ac.jp.

0272-8842/$36.00
doi:10.1016/j.ceramint.2009.03.038

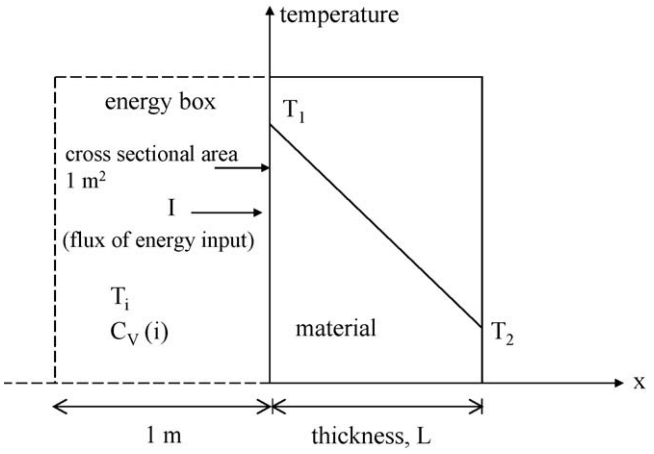

Fig. 1. Temperature difference in the solid material with thickness L at a given flux of energy. T_i and $C_v(i)$ represent the temperature and specific heat of material in the energy box with 1 m^3 volume at the left side of solid material, respectively.

value. The κ value is related to a specific heat (C_V, J/m^3K) under a constant volume and α by Eq. (3).

$$\kappa = \tfrac{1}{3} C_V \alpha \tag{3}$$

C_V and α are independently measured and the product of both the parameters provides κ. The temperature difference ($\Delta T = T_1 - T_2$) is discussed at the steady-state condition. (i) For a constant I value

$$\Delta T = T_1 - T_2 = \frac{IL}{\kappa} \tag{4}$$

The temperature difference becomes small at a high κ at a given thickness of material. Since T_2 is usually higher than room temperature (T_0), the following relation is derived.

$$T_1 \geq T_0 + \frac{IL}{\kappa} \tag{5}$$

T_1 becomes lower at a higher κ. (ii) For a constant T_1 from Eq. (5), the maximum flux of energy (I_{max}) conveyed through the solid material is limited by Eq. (6) at a given temperature difference ($T_1 - T_0$).

$$I_{max} = \frac{\kappa(T_1 - T_0)}{L} \tag{6}$$

When the energy (I) input is smaller than I_{max}, all the energy is conveyed through the material. However, when I is larger than I_{max}, the energy corresponding to the difference of both the I values ($\Delta I = I - I_{max}$) remains in the energy box in Fig. 1. A cubic box with 1 m^2 cross sectional area and 1 m thickness is assumed as an energy box. The energy produced per m^2 of solid material (H, J/m^2) during t seconds is given by $H = It$. The energy stored in the energy box is given by Eq. (7).

$$\Delta H = t(I - I_{max}) = t\Delta I \tag{7}$$

This energy enhances the temperature of the energy box as presented by Eq. (8),

$$\Delta H = \int_{T_1}^{T_i} C_V(i)\mathrm{d}T \cong C_V(i)(T_i - T_1) \tag{8}$$

Where $C_V(i)$ is the specific heat of the material in the energy box and treated as a constant value in Eq. (8). The combination of Eqs. (7) and (8) gives the time dependence of T_i (temperature of energy box) at a constant T_1 (Eq. (9)).

$$T_i = T_1 + \frac{\Delta I t}{C_V(i)} \tag{9}$$

When $C_V(i)$ is large, the increasing rate of T_i is small.

3. Thermal conductivity of laminated composite

3.1. Series flow of energy

Fig. 2 shows the laminated composite where a flux of energy (I) is input. At the steady-state condition ($I = I_1 = I_2$), the following equation is derived,

$$I = \kappa_1 \frac{T_1 - T_x}{L_1} = \kappa_2 \frac{T_x - T_2}{L_2} \tag{10}$$

where T_x is the temperature at the interface between layers 1 and 2. Eq. (11) gives T_x by solving Eq. (10),

$$T_x = \frac{(\kappa_1/L_1)T_1 + (\kappa_2/L_2)T_2}{(\kappa_1/L_1) + (\kappa_2/L_2)} = \frac{C_1 T_1 + C_2 T_2}{C_t} \tag{11}$$

where C_1, C_2 and C_t represent κ_1/L_1, κ_2/L_2 and $(\kappa_1/L_1) + (\kappa_2/L_2)$, respectively.

Substitution of Eq. (11) for Eq. (10) results in Eq. (12).

$$I = I_1 = I_2 = \frac{C_1 C_2}{C_t}(T_1 - T_2) \tag{12}$$

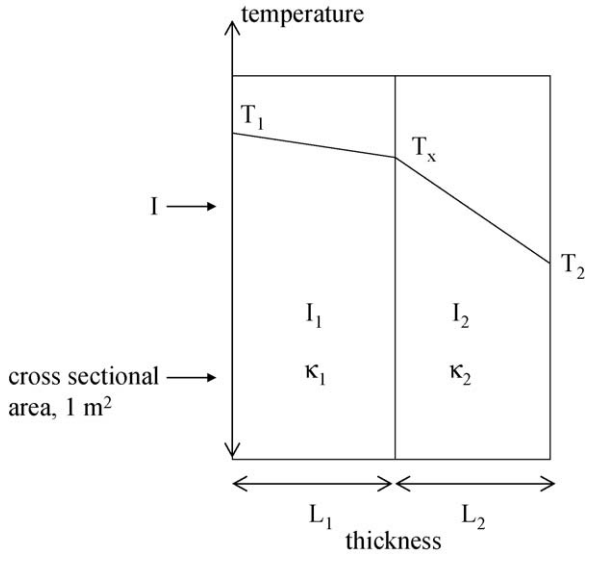

Fig. 2. Laminated composite consisting of two layers with different thermal conductivities and thickness.

The apparent thermal conductivity of the laminated composite (κ_C) is given by Eq. (13) and equal to Eq. (12).

$$I = \kappa_C \frac{T_1 - T_2}{L_1 + L_2} = \frac{C_1 C_2}{C_t}(T_1 - T_2) \tag{13}$$

As a result, κ_C is expressed by Eq. (14),

$$\kappa_C = \frac{C_1 C_2}{C_t}(L_1 + L_2) = \frac{\kappa_1 \kappa_2}{\kappa_1 l_2 + \kappa_2 l_1} \tag{14}$$

where l_1 and l_2 represent $L_1/(L_1 + L_2)$ and $L_2/(L_1 + L_2)$, respectively. For the condition of $\kappa_1/L_1 \gg \kappa_2/L_2$, κ_C is approximated to be Eq. (15).

$$\kappa_C \cong \frac{\kappa_2}{l_2} \tag{15}$$

The κ_C is dominated by the lower κ_2 value. When the number of layer is increased as seen in Fig. 3, the flux of energy is expressed by Eq. (16),

$$I = \tfrac{1}{2}(I_1 + I_4) = \tfrac{1}{2}(I_2 + I_3) = \frac{1}{2}\frac{C_1 C_2}{C_t}(T_1 - T_5) = \kappa_C \frac{T_1 - T_5}{2(L_1 + L_2)} \tag{16}$$

The derived κ_C is completely same as Eq. (14) and is not influenced by the number of layers.

3.2. Parallel flow of energy

Fig. 4 shows the parallel flow of energy toward two layers with S_1 and S_2 of cross sectional area and thickness L. The temperature T_3 at $x = L$ is fixed for both the layers. The energy input in layers 1 and 2 is expressed by Eqs. (17) and (18) using I (J/sm^2), respectively.

$$\frac{IS_1}{S_1} = I = \kappa_1 \frac{T_1 - T_3}{L} \tag{17}$$

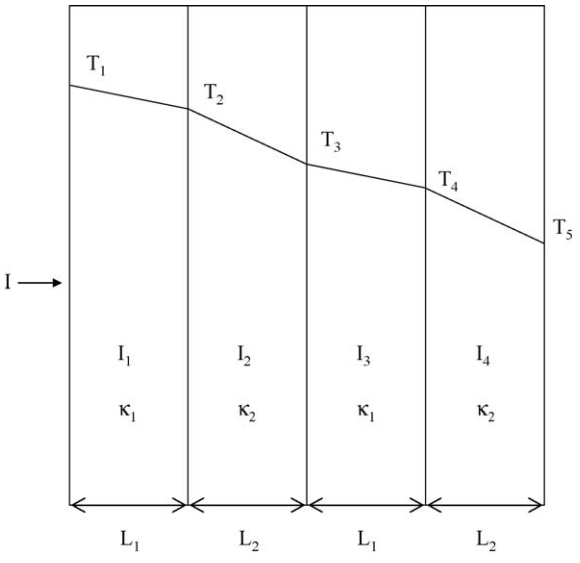

Fig. 3. Temperature difference in laminated composite consisting of four layers.

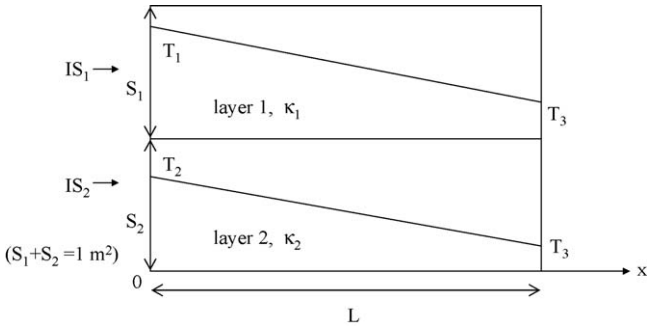

Fig. 4. Parallel flow of energy toward two layers with S_1 and S_2 of cross sectional area and thickness L.

$$\frac{IS_2}{S_2} = I = \kappa_2 \frac{T_2 - T_3}{L} \tag{18}$$

When κ_1 is higher than κ_2, T_2 becomes higher than T_1. This condition leads to the flux of energy from layer 2 to layer 1. After several seconds, the steady-state flow of energy provides the constant temperatures of T_h (high temperature) and T_l (low temperature) at $x = 0$ and L, respectively, for both the layers. The energy input to two layers ($S_1 + S_2 = 1$ m^2) during t seconds after the achievement of steady-state is expressed by Eq. (19).

$$H = It = t(S_1 + S_2)I = ItS_1 + ItS_2 \tag{19}$$

On the other hand, ItS_1 and ItS_2 are given by Eqs. (20) and (21), respectively.

$$ItS_1 = \left(\kappa_1 \frac{T_h - T_l}{L}\right) tS_1 \tag{20}$$

$$ItS_2 = \left(\kappa_2 \frac{T_h - T_l}{L}\right) tS_2 \tag{21}$$

Summation of Eqs. (20) and (21) gives Eq. (22) for the laminated composites with an apparent thermal conductivity κ_C.

$$It(S_1 + S_2) = It = \left(\frac{T_h - T_l}{L}\right) t(\kappa_1 S_1 + \kappa_2 S_2) = \left(\frac{T_h - T_l}{L}\right) t\kappa_C \tag{22}$$

Therefore κ_C for the parallel flow of energy is represented by Eq. (23).

$$\kappa_C = \kappa_1 S_1 + \kappa_2 S_2 = \kappa_1 S_1 + \kappa_2(1 - S_1) = \kappa_2 + (\kappa_1 - \kappa_2)S_1 \tag{23}$$

The κ_C in Eq. (23) changes linearly with increasing S_1.

4. Thermal conduction model of material with inclusion

In chapter 3, we discussed two types of thermal conductivity of laminated composite for series and parallel flow of energy. These two models are effectively coupled to derive κ_a of

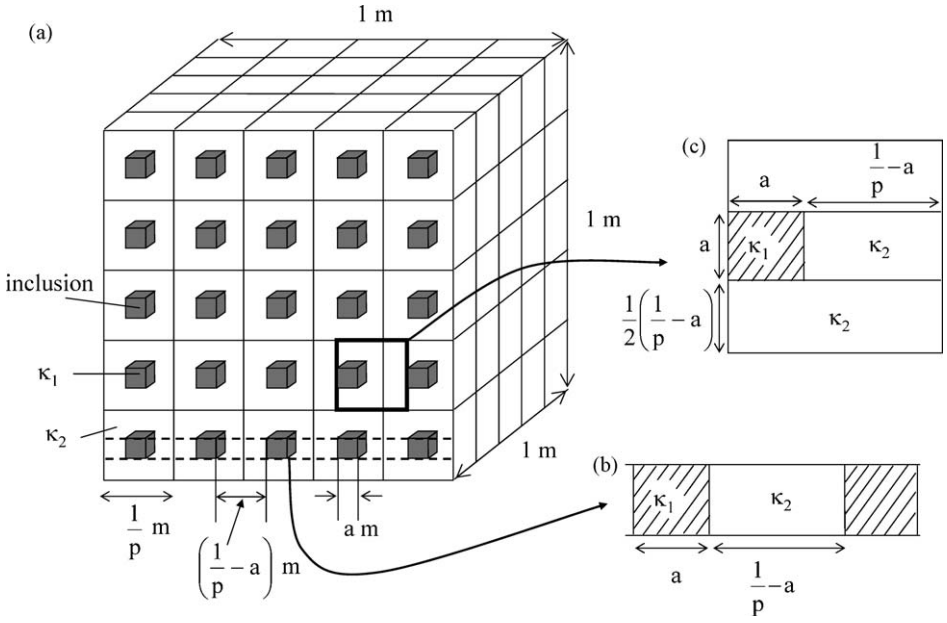

Fig. 5. A model structure of material with simple cubic inclusion with length a. The geometrical features are shown in Fig. 5 (b) and (c).

material with particulate inclusion. Fig. 5 shows a simple cubic inclusion model with a m length in one cubic box with length 1/p m. The number (n) and volume fraction (V) of cubic inclusion in 1 m^3 matrix box are related by Eq. (24),

$$V = a^3 n \tag{24}$$

The number (p) of inclusion along one direction of cubic matrix is equal to $n^{1/3}$ and the distance between two inclusion is given by $(1/p - a)$. The structure surrounded by dotted lines (Fig. 5 (b)) is same as the structure shown in Fig. 2. The L_1 and L_2 in Fig. 2 are changed to a and $(1/p - a)$, respectively. The apparent thermal conductivity (κ_{CP}) for the structure of Fig. 5 (b) is derived from Eq. (14),

$$\kappa_{CP} = \kappa_1\kappa_2 \frac{1}{C_t}\left(\frac{1}{a}\right)\left(\frac{1}{(1/p) - a}\right)\left(\frac{1}{p}\right) \tag{25}$$

the p value is given by Eq. (26) from Eq. (24).

$$p = \sqrt[3]{n} = \frac{V^{1/3}}{a} \tag{26}$$

Substitution of Eq. (26) for Eq. (25) provides Eq. (27).

$$\kappa_{CP} = \frac{\kappa_1\kappa_2}{C_t}\frac{1}{a}\frac{1}{1 - V^{1/3}} \tag{27}$$

The structure of Fig. 5 (b), whose κ_{CP} is expressed by Eq. (27), is sandwiched by two layers of a continuous matrix phase with a thermal conductivity κ_2. The geometrical lengths are shown in Fig. 5 (c). The structure of Fig. 5 (c) is basically same as the structure of Fig. 4. The layer 1 in Fig. 4 corresponds to the structure of Fig. 5 (b). That is, it is possible to understand the structure (c) with the model for the parallel flow of energy as shown in Fig. 4. The cross sectional area of matrix (S_{20}) surrounding one particulate inclusion is given by Eq. (28).

$$S_{20} = \left(\frac{1}{p}\right)^2 - a^2 = \left(\frac{a}{V^{1/3}}\right)^2 - a^2 = a^2\left(\frac{1}{V^{2/3}} - 1\right) \tag{28}$$

The number of inclusion per 1 m^2 is equal to $n^{2/3}$ and S_2 per m^2 is given by Eq. (29).

$$S_2 = n^{2/3}a^2\left(\frac{1}{V^{2/3}} - 1\right) \tag{29}$$

On the other hand the cross sectional area of particulate inclusion per m^2 is given by Eq. (30).

$$S_1 = n^{2/3}a^2 \tag{30}$$

Substitution of Eq. (26) for Eqs. (29) and (30) results in Eqs. (31) and (32), respectively.

$$S_2 = 1 - V^{2/3} \tag{31}$$

$$S_1 = V^{2/3} \tag{32}$$

The S_1 and S_2 correspond to S_1 and S_2 in Eq. (23), respectively. Similarly κ_1 in Eq. (23) corresponds to κ_{CP} in Eq. (27). The above relations are substituted for Eq. (23). Finally, the apparent thermal conductivity (κ_a) for the material with particulate inclusion is represented by Eq. (33).

$$\kappa_a = \kappa_2 - \kappa_2 V^{2/3}\left[1 - \frac{1}{1 - V^{1/3}(1 - (\kappa_2/\kappa_1))}\right] \tag{33}$$

The κ_a is related to κ_2 of a continuous phase, κ_1 of inclusion and V (volume fraction) of inclusion. The interesting feature is that no size effect of inclusion is seen in Eq. (33) and only V affects κ_a. Eq. (33) is compared with Eq. (34) which is derived based

Table 1
Characteristics and thermal conductivity of AlN–SiO_2 system hot-pressed at 1400–1600 °C.

Sample no.	Composition (vol. %)		Density (g/cm^3) (relative density, %)		Phases*	Thermal conductivity (J/smK)
	AlN	SiO_2				
1	23	77	2.20	85.2	C,A	2.49
2	23	77	2.46	96.4	C,A	7.10
3	40	60	2.24	82.9	C, A, SA	5.68
4	51	49	2.40	85.6	A, SA	8.15
5	69	31	2.70	91.0	A, SA	22.06
6	80	20	2.36	88.0	A, SA	28.34
7	90	10	2.71	74.9	A, SA	24.14
8	90	10	3.10	96.9	A, SA	29.27
9	95	5	3.03	94.3	A, SA	30.31
10	100	0	2.73	83.8	A, SA	37.79
11	100	0	3.20	98.2	A, SA	73.04

* C: SiO_2 (cristobalite), A: AlN, and SA: SiO_2·7AlN.

on the similarity to electrical conductivity [6].

$$\kappa_a = \kappa_2 \frac{1 + 2V[(1 - (\kappa_2/\kappa_1))/((2\kappa_2/\kappa_1) + 1)]}{1 - V[(1 - (\kappa_2/\kappa_1))/((\kappa_2/\kappa_1) + 1)]} \quad (34)$$

Eq. (34) leads to $\kappa_a = \kappa_2$ at $V = 0$ but κ_a becomes 3 κ_1 $(\kappa_1 + \kappa_2)/2$ $(2\kappa_2 + \kappa_1)$ at $V = 1$. On the other hand, κ_a of Eq. (33) results in $\kappa_a = \kappa_2$ at $V = 0$ and $\kappa_a = \kappa_1$ at $V = 1$. The thermal conductivity of the AlN–SiO_2 system was analyzed by Eqs. (33) and (34) in the next section.

5. Thermal conductivity of the AlN–SiO_2 system

AlN is known as an insulator of high thermal conductivity (320 J/smK) [4]. Dense AlN is produced by the liquid phase sintering with rare-earth oxide at a high temperature of 1800 °C. The κ of sintered AlN depends upon the oxygen content of starting powder and second phase at grain boundaries. On the contrary the κ of SiO_2 is as low as 2 J/smK [1]. In a previous paper [4], an AlN–SiO_2 composite powder was prepared by mixing an AlN powder (median size 1.4 μm) with tetraethyl orthosilicate. The precursor was hydrolyzed with moisture in air for 2 weeks–3 months to achieve uniform dispersion of AlN particles in SiO_2 matrix. The produced composite powder was hot-pressed without any sintering additives in a N_2 atmosphere at 1400–1600 °C. Table 1 shows the properties of the AlN–SiO_2 system hot-pressed at 1400–1600 °C. Relative density was in the range from 75% to 98% and increased when the hot-pressing temperature was increased. In samples 1, 2 and 3, AlN particles of 1–10 μm range were dispersed in a continuous cristobalite matrix. In samples 3–11, a part of AlN particles reacted with SiO_2 to form SiO_2·7AlN. This new phase (SiO_2·7AlN) was observed along the continuous grain boundaries between AlN grains. That is, the continuous phase changed from cristobalite to SiO_2·7AlN with increasing AlN composition.

Fig. 6 shows the AlN composition dependence of κ_a measured for the AlN–SiO_2 system. The measured κ_a increased nonlinearly with an increase in AlN content. The decrease in

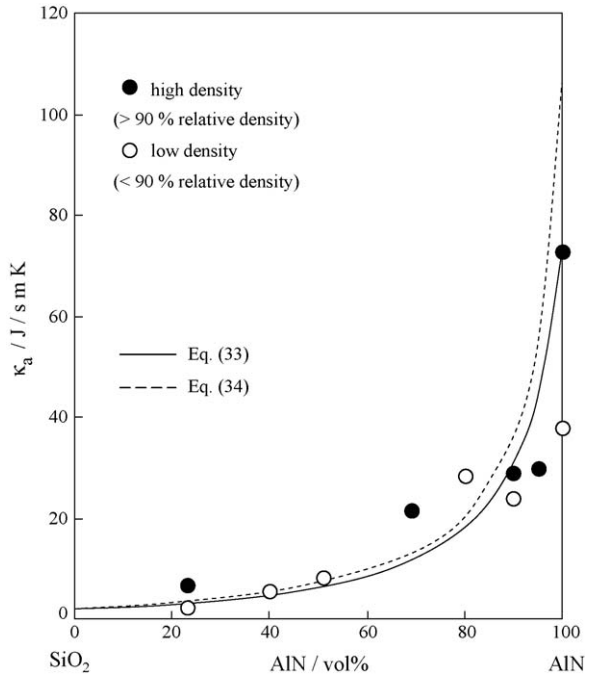

Fig. 6. Comparison between measured and calculated thermal conductivities for the AlN–SiO_2 system hot-pressed.

porosity leads to the increased κ_a at a similar AlN composition. The solid and dotted lines in Fig. 6 represent Eq. (33) and (34) with κ_1 (AlN) = 73.04 J/smK and κ_2 (SiO_2) = 2.00 J/smK, respectively. Both the lines express remarkably the tendency of κ_a measured. This good agreement may imply the similar κ values for SiO_2 and SiO_2·7AlN as a continuous phase. The difference of κ_a between Eqs. (33) and (34) becomes significant in the compositions near $V \approx 1$ as explained before. The above comparison between measured and calculated κ_a values concludes that the conduction model proposed in this paper (Eq. (33)), is effective to represent the measured thermal conductivity of material with particulate inclusion.

6. Conclusions

Thermal conductivity (κ_C) of the laminated composite consisting of two layers with different conductivities was analyzed for the series and parallel flow of energy. These two structure models and the derived κ_C equations are coupled to analyze the thermal conductivity (κ_a) of solid material with simple cubic particulate inclusion. The newly derived κ_a equation can be represented by κ_1 of inclusion, κ_2 of a continuous phase and volume fraction of inclusion, and was compared with the measured κ_a for the AlN particles-dispersed SiO_2 system. A very good agreement is shown for the measured and calculated κ_a values.

References

[1] K. Hata (Ed.), Chemical Handbook, Basic Part II, third ed., The Chemical Society of Japan, Maruzen, Tokyo, 1984, pp. 73–74.
[2] S. Nagasaki (Ed.), Metal Handbook, second ed., The Japan Institute of Metals, Maruzen, Tokyo, 1984, pp. 12–15.

[3] Y. Hirata, Thermal conduction model of metal and ceramics, Ceram. Int., accepted for publication.
[4] Y. Hirata, K. Nishikawa, Y. Fukushige, M. Tajika, Synthesis of AlN-dispersed oxide (silica, mullite) matrix composites by sol–gel method, Key Eng. Mater. 159–160 (1999) 353–358.
[5] K. Nishikawa, Synthesis of AlN-dispersed silica by sol-gel method, M.S. Thesis, Kagoshima University, 1999.
[6] W.D. Kingery, H.K. Bowen, D.R. Uhlmann, Introduction to Ceramics, second ed., John Wiley & Sons, New York, 1976 , pp. 612–643.